Emissions analysis of controlled environment agriculture in the Canadian Arctic

Banister, Carsen; Wills, Adam; Gallardo, Andres; Moore, Travis; Legaspi, Koreen; Martinussen, Nika

https://doi.org/10.4224/40003207

NRC·CNRC CONSTRUCTION

Emissions Analysis of Controlled Environment Agriculture in the Canadian Arctic

Author(s): Carsen Banister, Adam Wills, Andres Gallardo, Travis Moore, Koreen Legaspi, Nika Martinussen

Report No.: A1-019771.01
Report Date: 18 July 2023

National Research Council Canada | Conseil national de recherches Canada

Canada

(blank page)

Emissions Analysis of Controlled Environment Agriculture in the Canadian Arctic

Author

Banister, Carsen

Digitally signed by Banister, Carsen
Date: 2023.11.24 13:23:00 -05'00'

Carsen Banister, Ph.D.
Associate Research Officer
Integrated Building Performance
NRC Construction Research Centre

Approved

Zhou, Liang

Digitally signed by Zhou, Liang
DN: cn=Zhou, Liang, c=CA, o=GC, ou=NRC-CNRC, email=liang.zhou@nrcanada.ca
Date: 2023.12.14 10:19:08 -05'00'

Grace Liang Zhou, Ph.D.
Acting Research and Development Director
Building Performance and Quality
NRC Construction Research Centre

Report No: A1-019771.01
Report Date: 18 July 2023
Program: Intelligent Building Operations

50 pages

Copy no. 1 of 1

(This page is intentionally left blank)

Table of Contents

List of Figures

List of Tables

Executive Summary

Evidence presented in previous studies show that far-north Canadian populations face significant food security challenges, including quality, price, and availability of fresh fruits and vegetables. To target some of these challenges, several methods of protected agriculture have been attempted in recent years in high latitude locations in Canada. Although many studies show that it is feasible to produce quality fruits and vegetables in Controlled Environment Agriculture (CEA) facilities in the Arctic, there are concerns about the energy emissions from operating such facilities.

The high energy demand of CEA facilities and the high dependence on fossil fuels in the Canadian Arctic are factors that must be considered from a greenhouse gas emissions perspective. Thus, the objective of this study is to estimate the carbon dioxide equivalent emissions associated with the production of fruits and vegetables in a CEA facility located in the Canadian Arctic. Specifically, this study aims to answer the following research question: what is the relative quantity of greenhouse gases emitted for produce grown locally in the Arctic in a CEA facility compared to produce transported in from southern Canada?

The carbon dioxide equivalent footprint of produce cultivated in southern Canada was quantified based on previous studies and the emissions of air transportation of food were estimated based on two transportation paths from southern Canada to locations in the Canadian Arctic. The emissions associated with food produced in the Arctic were estimated based on modelling of the energy use of a CEA facility located in Cambridge Bay, Nunavut. Considering that the production of fruits and vegetables varies significantly depending on the type of produce and the referenced study, three different yield values (low, high, and average production) were selected for performing a sensitivity analysis of the total CEA emissions.

Cases of on-site renewable energy for CEA at increasing scales were modelled and compared to a baseline model with no renewable generation. The results of this study indicate that emissions from produce grown locally in the Arctic in a CEA facility could be at least eight times that of the emissions associated with products shipped from southern Canada if no local renewable generation is used.

Several factors could change this result – the use of renewable energy resources and more efficient production practices would reduce the emissions associated with CEA in these locations. Further, the transportation analysis did not look at the most extreme routes, such as the northernmost communities, which would increase the transportation carbon dioxide equivalent emissions, although likely only by a factor of two or three at most. While the societal needs for the supply of fresh food is more complex than just examining the related greenhouse gas emissions, this study indicates that until there is a significant proportion of renewable energy readily available in Canadian Arctic locations, CEA operated in these locations would likely result in significantly higher emissions per mass of food produced than air transport of food from lower latitude locations.

1 Introduction

Food insecurity is a complex and interdisciplinary topic for Arctic communities. Inuit and other Indigenous people have sustained themselves from their surrounding natural environments for millennia. Although country food (food harvested from the surrounding environment) remains an important part of the diet for cultural, access, self-reliance, and cost reasons, grocery store food became another important source of food in the Arctic over the 20th century. Given that polar climates are incompatible with most farming food production, food other than country food is transported in from southern Canada. Non-perishable foods are shipped via sea lift as much as possible and perishable foods are transported via air. This causes food costs at stores in the Arctic to often be at least double or triple that of the cost in southern Canada (CBC News, 2022).

Chan et al. (2006) presented evidence showing that far-north Canadian populations face poor quality of fruits and vegetables, along with high prices and periodic unavailability. As a result of these challenges, protected agriculture has been explored in recent years to increase the quality, affordability, and security of nutritious food in Canada's Arctic. This study is focused on the technology of controlled environment agriculture (CEA), which offers complete control of the grow enclosure. However, due to the high reliance on fossil fuels for heat and electricity in remote northern locations within Canada, the energy demands, costs, and associated greenhouse gas (GHG) emissions are of concern when considering CEA.

The majority of existing studies focusing on solutions for the production of fruits and vegetables in extreme environments do not report the carbon footprint of these products. As there is no information on the amount of CO_2 emissions from this type of facility, it is difficult to determine whether this process has a greater or lesser environmental impact than the alternative of air transport of food from southern Canada. To fill this gap, this work attempts to quantify the operational carbon emissions associated with the production of fruits and vegetables in a CEA facility located in the Arctic. The estimated emissions are compared with emissions from transporting an equal weight of fresh produce by airplane from southern Canada. Additionally, this study estimates the reduction in carbon emissions that can be obtained in CEA facilities by using energy generated on-site through small wind turbines or solar photovoltaic (PV) panels. The study is not intended to be a life cycle assessment (LCA) of either long range food transport or greenhouse vegetable production because both activities entail operations and energy terms that are beyond the scope of this study.

Section 2 presents a literature review of studies that focus on estimating emissions from food (fruits and vegetables) produced in CEA facilities or greenhouses located in cold climates. The methodology that was used to estimate emissions from Arctic CEA facilities and emissions from food transported by air from southern Canada is presented in Section 3. The estimated carbon footprint for each of the selected scenarios is presented in Section 4. This section also presents the different renewable energy generation scenarios that were evaluated for the CEA case. Finally, a summary and the conclusions of the study are presented in Section 5.

1.1 Greenhouse Gas Emissions Calculations

GHG emissions are of concern due to the greenhouse effect of the Earth's atmosphere, which refers to the capture and retention of heat energy from solar irradiation reaching the planet. Since gases in the atmosphere interact with radiation reflected and emitted by the Earth, the changing composition of gases in the atmosphere are affecting the balance of heat retained by Earth and its atmosphere. Since carbon dioxide (CO_2) is by far the most significant greenhouse gas by emissions mass, it is commonly used as a reference for quantifying the strength of other compounds as carbon dioxide equivalent ($CO2_e$). The relative strength of other compounds to CO_2 are expressed as global warming potentials (GWPs). As a result of many compounds decaying over time in the atmosphere, a time horizon for integrating the climate forcing of compounds is necessary to calculate their GWPs, with 20 and 100 years commonly used, but other time horizons can be used.

2 Literature Review

The literature review addresses two issues for arctic food production: what is the current knowledge on strategies for fresh food production in the Arctic and what models exist for estimating the GHG emissions resulting from food production. For food production in southern Canada, the literature review focussed on GHG emissions from both field and greenhouse production approaches, with the purpose being for comparison to emissions estimates for food production via CEA in the Canadian Arctic. Literature on renewable energy systems for CEA are also summarized.

2.1 Strategies for Local Fresh Produce Growth in Northern Canada

The most commonly reported protected agriculture method used in the Canadian north is greenhouses (McCartney and Lefsrud, 2018). Although greenhouses have a variety of designs, they are typically constructed with a glazed side oriented towards the equator and an opaque opposite side. Such designs rely on direct solar energy to heat the greenhouse during the day, and store energy via thermal mass to use during the colder night periods. An example of this system was evaluated in the study by Beshada et al. (2006), in which a greenhouse with an insulated solid north wall and a thermal blanket system was designed in Eli, Manitoba. The results of this study showed that greenhouse heating requirements can be very high, which can increase production costs and affect the sustainability of these projects.

In order to reduce the heating energy requirements of greenhouses located in cold climates, some studies have evaluated the use of double-wall rigid sheets of acrylic or polycarbonate materials (McCartney and Lefsrud, 2018). The use of these thermal screens has resulted in energy savings, but has some drawbacks such as increased relative humidity during overnight use and restrictions of daytime sunlight even when retracted (O'Flaherty and Maher, 1987). Another important drawback is that typical glass and film greenhouse materials do not have structural and thermal resistances suited for large snow loads and high winds. To overcome the

main challenges of greenhouses in cold climates, many studies have considered the use of fully closed systems.

The study of space-based life support systems, which provide fully controlled environments, has been of great importance for technology transfer applied to terrestrial greenhouse production in polar climates (Bamsey et al., 2009). Extraterrestrial technology is usually tested in polar conditions on Earth, as they share similar conditions in terms of cold temperatures, low light levels, and remoteness (Bucklin et al., 2001). For example, the Haughton Mars Project's Arthur Clarke Mars Greenhouse (ACMG) in the Canadian High Arctic has supported extreme environment related research for many years (Giroux et al., 2006). A group at the German Aerospace Center developed a shipping container-style closed system named the Eden ISS that was deployed at the Neumayer III station in Antarctica in late 2017 (Zabel et al., 2015). Other systems, such as that presented by Guo et al. (2008) and Bucklin et al. (2001), also show solutions for plant growth in extreme environments based on extraterrestrial plant growth requirements. The literary review conducted by Zabel et al. (2016) summarizes the progress made in this area during the last decades. In summary, the analysis conducted by Zabel et al. (2016) indicates that one of the main disadvantages of closed systems is the high electricity demand for lighting, despite the advances in LED technology efficiency. Additionally, the analysis highlights the limitations in terms of availability in the cultivation area, which can affect production capacity.

Avard (2015) studied the potential of northern greenhouses as a key approach for addressing food security in Inuit communities, particularly through the Kuujjuaq Greenhouse Project in Nunavik. While the research excludes technical and economic implications of northern greenhouse development, it explores their development through the lens of environmental sustainability, cultural fitness, and communal growth to address the cultural food security needs of Inuit communities. Results indicate positive impact in food security, sustainability, and socioeconomics and demonstrate the interest and need for northern greenhouses and agriculture for food sovereignty and resilience in the North. Sipola (2019) illustrated the social, nutritional, and ecological impact of local food systems in Indigenous, Arctic communities made by Northern gardens and greenhouses. Through a case study of a greenhouse development in Kuujjuaq, Nunavik, Sipola examined the environmental and sustainable challenges of greenhouse development, including the required air transport of soil and use of fossil fuels for greenhouse heating. Chen and Natcher (2019) developed an inventory of and examined 36 community gardens and 17 greenhouses across Northern Canada. A subset of these projects was highlighted to demonstrate their benefits, including local food production and skill development in the community. The community gardens and greenhouses discussed in the study performed by Chen and Natcher (2019) are an example of an effective strategy for food sovereignty because of the reduced dependency on expensive, nutrient-poor food imports and ability to satiate food needs in their respective communities.

There is a high interest in local food production in the Canadian Arctic due to the high costs and reduced quality of food flown in from the south. Various techniques to meet this desire have been used and studied, such as traditional greenhouses and CEA. To date, the majority of

studies have focused on the former, whereas there has been limited study of CEA energy performance and possibly no study of CEA emissions related to energy use.

2.2 Non-Arctic Produce Yields, Energy Intensity, and Emissions

2.2.1 Field Cultivation Emission

Various studies, in both Canadian and international contexts, have attempted to quantify the greenhouse gas emissions from field-grown fruits and vegetables. In a study by Dyer and Desjardins (2018), the Fruit and Vegetable Energy (FAVE) model was developed in order to estimate the energy usage and carbon emissions of the Canadian fruit and vegetable industries. The data for the various emission calculations came from data collected from fruit and vegetable grower focus groups in Nova Scotia and Southwestern Ontario. Yield data for this study, including production quantities and land use, were taken from Statistics Canada Socioeconomic Data (formerly known as CANSIM). Energy usage and carbon emissions were estimated for the 31 vegetables and 18 fruits documented in the Statistics Canada Socioeconomic Data. For the development of the cultivation energy-estimating algorithm, these crops were divided into commodity groups: six for vegetables, five for fruits, and one for potatoes.

Carbon emissions were estimated for six aspects of fruit and vegetable cultivation: field operations, nitrogen fertilizer supply, irrigation, the cooling of produce during on-farm storage, building maintenance and off-farm transport (by farm-owned vehicles).

The field operations carbon emissions included emissions from seed bed preparation tillage, seeding, cultivating for weeds, spraying, harvesting, and carting the produce from the field to on-farm storage sites. The emissions produced by the various machinery involved in these processes were derived directly from the Fossil Fuel Farm Fieldwork Energy and Emissions (F4E2) model, developed by Dyer and Desjardins in 2003.

The nitrogen fertilizer supply emissions included converting the required amount of nitrogen fertilizer to be applied to the various crops, to the equivalent amount of natural gas used in the manufacturing process of the fertilizer. The amount of methane released from the use of natural gas in the production of the fertilizer was also considered and converted into carbon dioxide equivalent emissions.

Information collected from focus groups was used to estimate emissions from irrigation. Producers reported that a rate of 400 gallons of water per minute for one hour provides approximately one acre inch of water and requires approximately two gallons of diesel fuel to power the irrigation pumps. This translates to 11.3 m^3 of water per litre of diesel fuel (Dyer and Desjardins, 2018). Rates of irrigation data by province and farm type from Statistics Canada were used with the above rate of diesel fuel consumption to estimate carbon emissions from irrigation.

To estimate on-farm cooling, storage space required for a tonne of produce was calculated and converted to required energy use from crop yield data from Statistics Canada and known conversion factors between e.nergy use and storage space. Energy use was then translated to

carbon emissions using an electrical power to carbon emissions conversion factor developed by taking a weighted average from the proportions of energy system carbon emissions by the vegetable production of each province.

Finally, emissions produced by buildings and off-farm transportation were indexed directly from the 1996 Farm Energy Use Survey by Natural Resources Canada.

Taking these various methodologies to estimate emissions of the various produce cultivation activities, the Fruit and Vegetable Energy model was developed by Dyer and Desjardins (2018), and produced the estimates of carbon emissions shown in Table 1, separated by region and crop. As the source does not clarify if non-CO_2 GHGs are included, it is assumed that only CO_2 emissions are included in these figures.

Table 1. CO_2 emission rates for 12 selected crops in the four major vegetable and fruit growing provinces of Canada on an area and weight of product basis for the average 2007 to 2016 period (Dyer & Desjardins, 2018).

Region/ Province	AP	QC	ON	BC	AP	QC	ON	BC
Produce	**Area-Normalized Emissions** [tonne CO_2/ha]				**Yield-Normalized Emissions** [tonne CO_2/tonne crop]			
Vegetables								
Carrots	1.76	1.80	1.84	1.85	0.04	0.05	0.04	0.08
Sweet corn	1.30	1.35	1.39	1.40	0.24	0.13	0.11	0.19
Tomatoes	2.43	2.47	2.51	2.52	0.22	0.14	0.03	0.12
Peas	0.92	0.96	1.00	1.01	0.40	0.22	0.22	0.20
Lettuce	1.48	1.52	1.56	1.57	0.25	0.07	0.11	0.06
Cabbage	1.86	1.90	1.72	1.95	0.07	0.05	0.06	0.09
Fruits								
Apples	1.42	1.21	1.03	1.25	1.00	1.22	0.29	0.21
Peaches	1.34	1.13	1.07	1.13	0.11	0.00	0.12	0.09
Blueberries	1.52	1.26	1.04	1.44	0.07	0.06	0.04	0.05
Strawberries	1.36	1.10	0.88	1.08	0.25	0.17	0.17	0.20
Grapes	0.95	0.89	0.82	0.86	0.26	0.32	0.09	0.13
Potatoes								
Potatoes	1.19	1.17	1.14	1.10	0.04	0.04	0.05	0.03

Where AP refers to Atlantic Provinces, QC refers to Quebec, ON refers to Ontario, and BC refers to British Columbia.

A systematic review of greenhouse gas emissions from the production of different fresh foods by Clune et al. (2017) synthesized the available data on global warming potentials produced through agriculture. In total, 369 published studies with 1718 global warming potential (GWP) values for 168 varieties of fresh produce were reviewed. There was also global representation from where the data were collected, with most studies taking place in Europe, Oceania, and North America. To more accurately compare the studies, the system boundary was set to be from the activities and processes of the farm to the transportation of the produce to the regional distribution centre; emissions data were adjusted according to the set review boundary. Studies that did not include the system boundary or did not report emissions according to their life cycle stage were excluded. Emission sources considered were chemicals and fertilizers, fuel and

energy inputs from irrigation and machinery for cultivation, harvesting and processing, transport and refrigeration to the regional distribution centre, and emissions released from fertilized soils, plants and animals in fields. However, no post-processing methods were applied to the data to align the methods by which each of the studies came to reach their emissions estimates. A summary of the statistical analysis completed for classifications of various produce reviewed in this study is presented in Table 2. The normalized emissions are presented in units of kg CO_2e per kg produce yield.

Table 2. Fruit, vegetable and staples normalized emissions values [kg CO_2e/kg produce] (Clune et al., 2017).

Classification	Foods included	Median	Mean	Standard Deviation
Brassica	Cabbages, other brassicas	0.23	0.32	0.30
Bulbs, roots and tubers	Onions, garlic, beetroot, swedes and carrots	0.18	0.21	0.12
Leaves	Varieties of lettuce	0.37	0.38	0.14
Vegetables	Vegetables (all field grown vegetable)	0.37	0.47	0.39
Stem shoots	Asparagus	0.83	0.92	0.49
Brassica	Broccoli and cabbage	0.50	0.57	0.33
Pome	Apples, pears and quinces	0.29	0.34	0.18
Pepo	Fruit of the gourd family	0.30	0.34	0.29
Hesperidium	Fruits of the citrus family	0.33	0.35	0.12
Fruit	Fruits (all field grown fruit)	0.42	0.50	0.32
Drupe	Stones fruits	0.45	0.57	0.36
Multiple fruit	Pineapples and figs	0.45	0.68	0.50
True berry	Tomatoes, grapes, avocado, peppers, kiwi fruits, guava etc.	0.45	0.52	0.26
Aggregate fruit	Strawberries and raspberries	0.60	0.66	0.35
Musa	Bananas	0.72	0.79	0.30

Poore and Nemecek (2018) also completed a systematic review of the environmental impacts of food production. This analysis included 570 studies, which resulted in a data set of approximately 38,700 commercially-viable farms. The system begins with the extraction of resources required for agricultural production, the farm practices and activities, and ends at the market. Six emissions stages were considered: land use change, on-farm emissions, processing, packaging, transportation, and retail. For this study, land use change included four emission sources, including above ground carbon stock change, below ground carbon stock change, forest burning, and organic soil burning. Most studies do not include GHG emissions from land use change, so these emissions sources were estimated. Parameters include country-specific data on agricultural land expansion data by country, coupled with above-ground and below-ground carbon. Organic soil and forest burning emissions estimates were also derived from country-specific data. A summary of the mean and median emissions for various classifications of produce found by Poore and Nemecek (2018) are presented in Table 3.

Table 3. Estimated GHG emissions of vegetables and fruits [kg CO_2e/kg produce] (Poore and Nemecek, 2018).

Produce	Mean	Median
Tomatoes	2.1	0.7
Root vegetables	0.4	0.4
Brassicas	0.5	0.4
Berries and grapes	1.5	1.4

Table 4 summarizes the stages of greenhouse gas emissions considered in each of the studies. From this table, it is evident that Poore and Nemecek (2018) included the broadest scope for emissions related to vegetable and fruit production, whereas Desjardins and Dyer (2018) considered the smallest scope. While the emissions estimates understandably vary widely for a given type of produce, these three sources do generally corroborate each other in terms of the order of magnitude of emissions. For example, tomatoes have a mean value of 2.1 kg CO_2e/kg produce according to Poore and Nemecek, but the value is much lower for the other two sources, at 0.03 to 0.22 kg CO_2e/kg from Dyer and Desjardins and 0.45 kg CO_2e/kg from Clune et al. For greenhouse cultivated produce, it can be expected that the CO_2e emissions are likely much greater than for field cultivated produce, which may be the case with these differences for Tomatoes. In any case, nearly all of the data indicate less than 1 kg CO_2e/kg produce, with the maximum overall being tomatoes at 2.1. This serves as a good basis for comparison to the emissions estimated for CEA by this study.

Table 4. Stages of greenhouse gas emissions considered in different studies.

Emission stage considered	Poore and Nemecek, 2018	Clune et al., 2016	Desjardins and Dyer, 2018
Land use change	✓		
Crop production and harvest	✓	✓	✓
Processing	✓	✓	
Packaging	✓	✓	
Transport to regional distribution centre	✓	✓	✓
Retail	✓		

2.2.2 Greenhouse Cultivation

2.2.2.1 Greenhouse fruits and vegetables production in Canada

According to the 2021 Greenhouse, sod and nursery industries tables from Statistics Canada, the principal crops grown in Canadian greenhouses are tomatoes, cucumbers, peppers, and lettuce. As shown in Figure 1, these vegetables accounted for more than 98% of the total greenhouse fruits and vegetables production in 2021.

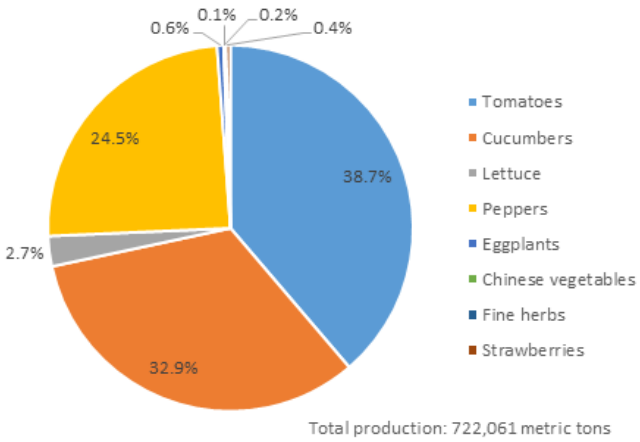

Figure 1. Breakdown of the total greenhouse fruits and vegetables production for the year 2021 (Statistics Canada, 2023. Table 32-10-0456-01)

Table 5 summarizes the information from Table 32-10-0456-01 Production and value of greenhouse fruits and vegetables by Statistics Canada for the 2017-2021 period, which includes harvested area and production by weight. With this information, a total yield between 36 to 44 kg/m^2 was calculated for all vegetables. The calculated range is slightly lower than the value reported in the study by Dyer et al. (2011) for all Vegetables in Canada (47 kg/m^2 – averaged over years 2002 to 2007).

Table 5. Production amounts of common greenhouse fruits and vegetables in Canada. (Statistics Canada, 2023. Table 32-10-0456-01)

Produce Type	Parameter	2017	2018	2019	2020	2021
Fresh tomatoes	Area harvested (10^6 m^2)	6.36	6.58	6.35	6.18	6.84
	Production (10^6 kg)	279	279	265	258	280
	Total yield (kg/m^2)	44.0	42.5	41.7	41.7	40.9
Fresh cucumbers	Area harvested (10^6 m^2)	4.32	4.56	4.74	5.06	4.67
	Production (10^6 kg)	206	229	232	253	238
	Total yield (kg/m2)	48	50	49	50	51
Fresh lettuce	Area harvested (10^6 m^2)	0.209	0.236	0.417	0.344	0.335
	Production (10^6 kg)	6.26	7.05	11.84	15.14	19.22
	Total yield (kg/m^2)	30	30	28	44	57
Fresh peppers	Area harvested (10^6 m^2)	5.63	5.62	5.76	5.90	6.79
	Production (10^6 kg)	139	139	146	152	177
	Total yield (kg/m^2)	25	25	25	26	26
All vegetables	Total yield (kg/m^2)	37	37	36	40	44

Using a greenhouse test facility located near the German Neumayer III station in Antarctica, Zabel et al. (2020) obtained an overall yearly productivity of around 27.4 kg/m^2 during the 2018 season. Although this productivity may seem low compared to other referenced values, it should be noted that this study is the only one that reports the production of a greenhouse located in Antarctica.

2.2.2.2 Energy use intensity of greenhouses and CEA in Canada

The study performed by Dyer et al. (2011) provide estimates of the energy and CO_2 emissions from vegetable greenhouses in Canada. Based on an average vegetable yield of 47 kg/m^2 and a total energy consumption of 6.77 PJ, the results of this study suggest that the average energy consumption of greenhouses in Canada is around 4.42 kWh/kg. The vegetable yield reported in the study was obtained from the 2002-2007 Greenhouse, Sod and Nursery Industries catalogue published by Statistics Canada. The total energy consumption of greenhouses was estimated with a simplified greenhouse heat loss calculation and the electrical energy use index proposed by Dyer and Desjardins (2006).

A joint project between Agritecture LLC and WayBeyond Ltd. recently published the 2021 Global CEA census report, which included a focus on the energy consumption of the CEA industry. As shown in Figure 2, the energy use per kilogram of product reported in the census shows a high variation, with more than 50% of farms having an energy use under 10 kWh/kg and 20% using under 1 kWh/kg. However, responses that had much higher consumption rates were also reported, which increased the average. This resulted in a median of 5.4 kWh/kg and an average of 22.5 kWh/kg (Waybeyond 2021). Comparatively, the study performed by Barbosa et al. (2015) estimated an on-farm energy use of approximately 0.3 kWh/kg for lettuce, which illustrates the high energy intensity of CEA.

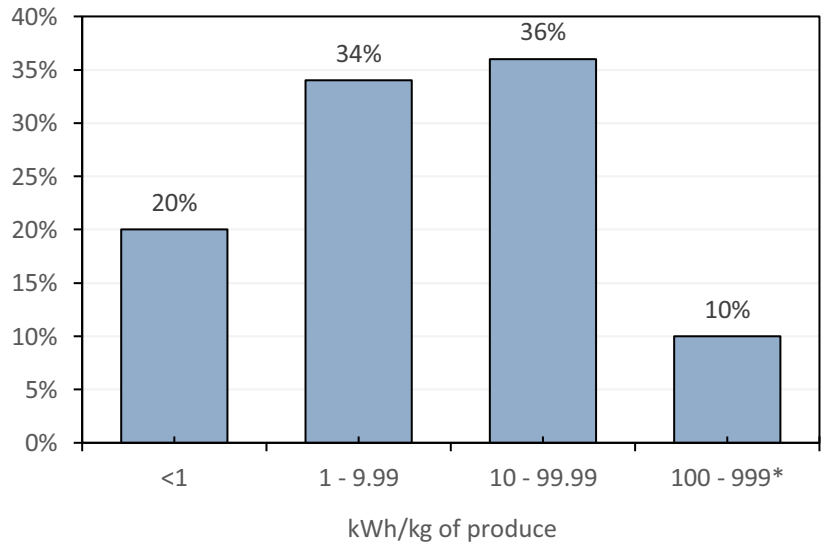

Figure 2. Responses to energy use per kilogram of product. Adapted from the 2021 Global CEA census report. *Responses in the 100 – 999 range include two major outliers.

Responses from the 2021 Global CEA census report also showed that smaller facilities (under 1000 m^2) have significantly higher energy use per kilogram of product compared to their larger counterparts (Figure 3). This indicates that small CEA facilities in the Arctic can be expected to have significantly higher energy and emissions intensities than larger facilities which may be located in lower latitudes.

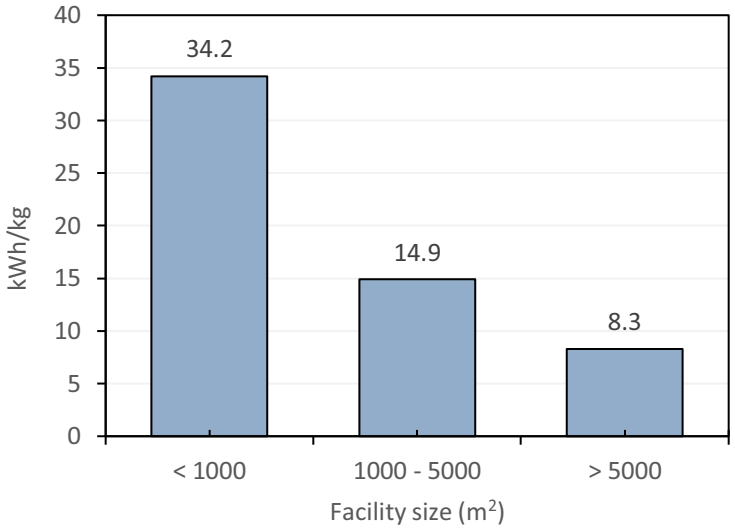

Figure 3. Energy use by facility size, adapted from the 2021 Global CEA census report.

2.2.2.3 Operational CO_2 emissions of greenhouses

There are only a few estimates in the literature of the carbon footprint of greenhouse fruits and vegetables. In the study performed by Dyer et al. (2011), emission intensities of 0.777, 0.770, 0.879 and 1.06 kg CO_2e/kg produce were obtained for Quebec, Ontario, Alberta and BC, respectively, and 0.851 kg CO_2e/kg produce for Canada. The carbon footprint estimates of greenhouse fruits and vegetables obtained by Stossel et al. (2012) are slightly higher. For cucumber production in heated greenhouses in Switzerland, a carbon footprint of around 2 kg CO_2e/kg produce was reported. The main driver of impact was greenhouse heating with fossil fuels during the winter and shoulder seasons.

2.3 Renewable Energy Solutions for CEA

Natural gas, oil, and biomass heating using water boilers and networks of piping are widespread in cold climate protected agriculture (Teitel et al., 1996; Chau et al., 2009); however, most of the Arctic regions do not have access to biomass or natural gas, and mainly rely on oil products for heating. This creates a significant quantity of emissions for produce growth in CEA facilities for these locations. One method to mitigate these emissions is through the use of renewable energy sources such as wind or solar photovoltaic. This section summarizes previous studies that have considered renewable energy integration.

Exner-Pirot (2012) argue that without access to natural gas, other energy sources such as wind and micro-nuclear power may provide cost effective sources of energy in Arctic regions. Sambor (2020) explored the optimization of a solar PV and battery system applied to a container farm of size 8 ft x 8 ft x 40 ft. A model was developed to optimize the operations of the solar PV and battery storage system and its capacity to power the loads of a container farm in a remote community. The electric loads considered in the model include: air circulation fans, water pumps, lighting, heating/cooling, ventilation/exhaust fan, and dehumidification. The model was applied under various simulation scenarios using collected load data from a container farm in the Yukon. Results indicated that a solar PV system providing 17kW of power to the container farm's loads was optimal and leads to a 14% decrease in annual cost for this scale of CEA.

In regions outside of Canada, similar analyses have been conducted. Karenzi (2020) developed energy distribution models using MATLAB's Simulink tool to demonstrate the interrelations and dynamics of renewable energy resources on food, energy, and water infrastructures in Arctic communities using a microgrid, particularly in Alaska. Ljungqvist (2021) proposed using excess heat from a data center as a heating source for producing tomato crops in 2,000 m^2 and 10,000 m^2 greenhouses in northern Sweden (65° north). A building energy model of the data center and the greenhouse was developed considering energy shades, lighting, temperature, transpiration, ventilation, and economic cost. Results of a building energy simulation conclude that for smaller greenhouse approximately 90% of the heat demand can be met from the data centre's excess heat and 55% for the larger greenhouse.

2.4 Summary

The literature review indicates that there are not many studies that report the emissions of Arctic CEA facilities. The information that is available in national statistics corresponds mostly to the carbon footprint of fruits and vegetables produced in the field or in greenhouses in the southern part of Canada. In this study, the yield data on greenhouse fruits and vegetables production is used to support estimating the emissions of Arctic CEA facilities. This assumption is appropriate since the crop productivity in CEA is expected to be more related to that in greenhouses than for field production. Table 6 summarizes the information collected on greenhouse production, energy use and emissions, from which the CEA emissions are estimated in the corresponding following section.

Table 6. Estimates of production, energy use intensity and carbon footprint of controlled environment agriculture facilities from different studies.

Study	Location	Fruits and vegetables production (kg/m^2)	Energy use intensity (per area) (kWh/m^2)	Energy use intensity (per kg) (kWh/kg)	Carbon footprint (kg CO_2e/kg of produce)	Type of produce	Growing environment	Lighting intensity (kWh/m^2)
GH Energy Profile study	Ontario	37.2	495.9	13.3	0.41*	All vegetables and fruits	Greenhouse	320
2021 CEA census report	Various countries	-	-	8.3 - 34.2	-	All vegetables and fruits	Various types	-
Dyer et al. (2011)	Canada	47.0	207.9	4.4	0.85	All vegetables and fruits	Greenhouse	34
Zabel et al. (2020)	Antarctica	27.4	-	-	-	Overall yearly productivity	Mobile test facility (container)	-
Katzin et al. (2021)	Anchorage, Alaska; Kiruna, Sweden	-	700 - 940	-	-	Not specified	Greenhouse	265 - 460
Stoessel et al. (2012)	Switzerland				2	Cucumbers	Heated greenhouse	-
Stats. Canada (2017 - 2021)	Canada	38.7	-	-	-	All vegetables and fruits	Greenhouse	-

* Assuming an annual average emissions factor of 0.031 kg CO_2e/kWh

3 Methodology

This section outlines the methodology used to estimate the emissions produced from two methods of supplying Arctic communities with produce: delivering fresh produce from southern Canada via air transport and growing produce locally in a controlled environment. This analysis enables a comparison of the carbon dioxide equivalent emissions of each scenario.

3.1 Estimating Emissions of Air Transport

The methodology that was used to estimate emissions from transporting fresh produce by airplane from southern Canada is not intended to be a Life Cycle Assessment (LCA), as there are several processes that are beyond the scope of this study. These processes include the production and transportation of equipment for southern cultivation, and surface transportation (from cultivation location to southern airport terminal and from Arctic airport terminal to distribution location). The methodology includes only the following processes:

- **Produce cultivated in southern location**
    - Can be traditional outdoor agriculture or greenhouse agriculture, with the latter typically having higher operational emissions.
- **Transportation from southern location to Arctic community**
    - Air transportation is the primary consideration and includes take-off, cruise, descent, and landing. There are a variety of aircraft types and routes travelled.
    - Surface transportation is included for cases where the origin airport is a northern location (e.g., Yellowknife)

The carbon footprint of produce cultivated in southern Canada is estimated based on the studies described in the literature review. However, it is important to note that the emissions from cultivation of produce vary widely across types and can also vary considerably across producers for the same type.

The transportation emissions per mass of produce transported are calculated based on the route travelled, aircraft used, and surface transportation distance if significant.

3.1.1 Air Transport Cargo Capacity

Volume and mass are the two considerations for the capacity of air transport of cargo. Aircraft have both volume and mass limitations based on their size, power, wing areas, and structure. Given this, it is necessary to evaluate whether certain types of produce will be volume-limited or mass-limited by the capacity of a given aircraft. The two aircraft considered later in this analysis are examined for this assumption, the Boeing 767-300F and the ATR 42, as they are common for the locations being considered. The cargo capacity density is first calculated to compute the maximum mass per volume of payload the aircraft can carry assuming all the volume is used. Payloads with higher densities than this will consume all of the mass payload capacity before the volume capacity and therefore be mass-limited. Payloads with lower densities than this will

consume all of volume payload capacity before the mass capacity and therefore be volume-limited. The cargo capacity densities of the aircraft are calculated according to Equation (1):

$$\rho_{cap,\text{aircraft}} = \frac{m_{cap,\text{ aircraft}}}{V_{cap,\text{ aircraft}}} \quad (1)$$

Where:

$\rho_{cap,\text{aircraft}}$ is the cargo capacity density of the aircraft,

$m_{cap,\text{ aircraft}}$ is the mass capacity of the aircraft, and

$V_{cap,\text{ aircraft}}$ is the volume capacity of the aircraft.

For the Boeing 767-300F:

$$\rho_{cap,767-300F} = \frac{52{,}700\ kg}{438\ m^3} = 120\,\frac{kg}{m^3}$$

(Boeing, 2014)

For the ATR-42:

$$\rho_{cap,ATR-42} = \frac{5580\ kg}{54\ m^3} = 103\,\frac{kg}{m^3}$$

(Bringer Air Cargo, 2021)

The produce density is calculated as in Equation (2):

$$\rho_{\text{produce, packed}} = \frac{m_{\text{produce, packed}}}{V_{\text{produce, packed}}} \quad (2)$$

Where:

$\rho_{\text{produce, packed}}$ is the density of the packed produce,

$m_{\text{produce, packed}}$ is the mass of the packed produce, and

$V_{\text{produce, packed}}$ is the volume of the packed produce.

Iceberg lettuce is chosen as a representative produce type; certain types of produce will be somewhat less dense and others somewhat denser. The mass of packed iceberg lettuce per 40

foot container is taken from the information of a producer/supplier at 11,160 kg (Cairo Fruit, 2021). The capacity of a 40 foot refrigerated container is approximately 59.3 m^3 (DSV, n.d.).

$$\rho_{\text{produce, packed}} = \frac{m_{\text{produce, packed}}}{V_{\text{produce, packed}}} = \frac{11{,}160\ kg}{59.3\ m^3} = 188.2\frac{kg}{m^3}$$

Given that the density of packed iceberg lettuce is greater than the cargo capacity densities of the aircraft considered, the freight will be mass-limited rather than volume-limited.

3.1.2 Flight Distance

To determine the fuel burned during the cruising portion of the flight, two calculations are required: the great circle distance [km] and time duration of flight [h]. The great circle distance, shown in Equation **Error! Reference source not found.**), is the shortest distance between two points along the surface of a sphere (in this case Earth) calculated using the longitude and latitude co-ordinates of the plane's origin and destination (Kells, L. et al., 1940). The central angle between the points on a sphere, $\Delta\sigma$, can be calculated as in Equation (3):

$$\Delta\sigma = \arccos(\sin\phi_1 \sin\phi_2 + \cos\phi_1 \cos\phi_2 \cos(\Delta\lambda)) \quad (3)$$

Where:

$\Delta\sigma$ is the central angle between the two points of interest on a sphere's surface,

ϕ_1, λ_1 are the geographical latitude and longitude of point 1, respectively,

ϕ_2, λ_2 are the geographical latitude and longitude of point 2, respectively, and

$\Delta\phi, \Delta\lambda$ are the absolute differences of latitude and longitude, respectively.

The arc length, d, on the surface of a sphere can be calculated according to Equation (4):

$$d = r\Delta\sigma \quad (4)$$

Where:

r is the radius of the sphere.

In practice, a 'great circle distance' calculator can be used to quickly compute the distance for a given flight between two locations, such as "Great Circle Mapper" (2023). Using the average cruise speed of an aircraft [km/h], the time travelled can then be calculated. Finally, considering

the average hourly rate of fuel burn of an aircraft [kg_{fuel}/h], the total fuel burned can be determined [kg_{fuel} or L_{fuel}].

The fuel burned is then doubled given that an aircraft delivering food to the Arctic must complete a round trip and the return trip is unable to make effective use of the cargo capacity.

3.1.3 Flight Emissions

Aircraft flights can be broken down into the following stages:

Taxi-out, take-off, climb-out, cruise, descent, approach, landing, taxi-in.

For emissions calculations purposes, the flight stages can be grouped into landing/take-off (LTO) cycles and cruise. LTO includes all activities below the altitude of 1000 m, including taxi-out and -in, take-off, climb-out, approach, and landing. Cruise includes all activities above the altitude of 1000 m, including climb to cruise altitude, cruise, and descent from cruise altitudes (IPCC, n.d.).

The following assumptions are applied to the analysis:

- Based on the calculations in Section 3.1.1, the freight is mass-limited as opposed to volume-limited for all produce. This means that the maximum mass payload of the aircraft is what is considered to be the freight amount, rather than the volumetric cargo capacity of the aircraft.
- 95% of the cargo capacity will be filled with produce, with packaging of negligible mass.
- Before arriving at the Arctic destination, the plane is not diverted back to Southern Canada (i.e., is able to deliver all produce to destination as planned).
- At all airports to be landed at, the plane is able to land without the need to hold in the air.
- The emissions to transport produce from the airport to the Arctic distribution location are negligible.

IATA Recommended Practice 1678 is used to estimate the CO_2e emissions for the cruise phase of the flight (including climb and descent) for the air transport of produce to Arctic locations (IATA, n.d.).

Emissions from combustion of jet A-1 fuel include CO_2, CH_4, N_2O, NO_x, CO, NMVOCs, and SO_2, among others (IPCC, n.d.). Total CO_2e from jet A-1 combustion by aircraft is heavily dominated by CO_2. For this analysis, only CO_2, CH_4, and N_2O are considered with emissions values from Canada's Greenhouse Gas Inventory shown in Table 7 (Government of Canada, n.d.). The CO_2e emissions from the CH_4 and N_2O emissions are determined using their respective 100 year Global Warming Potentials (GWPs), shown in Table 8. The volume of fuel is converted to mass of fuel using the density in Table 9.

Table 7. Aviation turbo fuel emission factors. (Government of Canada, n.d.)

Source	kg CO_2e / L Jet A-1 Fuel	kg CO_2 / L Jet A-1 Fuel	g CH_4 / L Jet A-1 fuel	g N_2O / L Jet A-1 fuel
Environment and Climate Change Canada GHG Inventory	2.58	2.56	0.018	0.0711

Table 8. Global Warming Potentials for a 100-Year Time Horizon (IPCC, n.d.)

Greenhouse Gas	CO_2	CH_4	N_2O
GWP	1	25	298

Table 9. Jet-A-1 fuel density (Air BP, 2000)

Jet A-1 fuel density	0.804 kg/L

Completing the calculations results in Equation (5) below for the carbon dioxide equivalent emissions per mass of fuel burned.

$$CO_2e \text{ Emissions} = \text{Total Mass of Fuel Burned} \times 3.21 \frac{kg_{CO_2e}}{kg_{fuel}} \quad (5)$$

3.2 Estimating Emissions of Surface Transport

Emission factors for surface transport vary widely depending on the type of truck and its use. Urban delivery trucks have the highest emissions factors, with one source estimating an average of 307 grams of CO_2 per ton-kilometre (g CO_2e/t-km), whereas long-haul tractor-trailers have the lowest emissions factor, estimated by the same source at an average of 57 g CO_2e/t-km. Given the majority of the surface transport required to move food for the purposes of this analysis will be by long-haul tractor-trailer, the emissions factor of 57 g CO_2e/t-km is used (International Council on Clean Transportation, 2021). This also serves as a lower bound for the emissions estimate.

3.3 Emissions of Arctic Controlled Environment Agriculture

This section outlines the methodology used to estimate the emissions produced from growing produce locally in a controlled environment. The proposed methodology is not intended to be a lifecycle assessment (LCA), as that would include operations and energy terms that are beyond the scope of this study (e.g., production and transportation of required materials to Arctic

location or transportation from CEA to distribution location). The methodology used by this study includes the following steps:

- Create a building energy model of the CEA facility and solve numerically
- Estimate the energy use intensity per kg of produce (kWh/kg)
- Estimate the average yield of greenhouse fruits and vegetables (kg/m^2)
- Calculate the operational CO_2e emissions per kg of produce (kg CO_2e/kg produce)

3.3.1 Production of CEA fruits and vegetables

The crop productivity of CEA is expected to align more closely to that for greenhouses than field production. For this reason, data on greenhouse fruits and vegetables production reported in the literature review was used to estimate the emissions of Arctic CEA. Three different yield values (low, mid, and high production) have been considered for performing a sensitivity analysis (Table 10).

Table 10. Average production of greenhouse fruits and vegetables in Canada for the 2017 – 2021 period. (Statistics Canada, 2023. Table 32-10-0456-01)

	Low	Mid	High
Crop type	Strawberries	Lettuce	Cucumber
Crop productivity (kg/m^2)	8	38	50

3.3.2 Energy use intensity of CEA

The energy use intensity per kilogram of produce (kWh/kg) was used as a metric of the energy consumption of a CEA facility. This metric can be calculated using Equation (6) as follows:

$$EUI\left(\frac{kWh}{kg}\right) = \frac{EUI\left(\frac{kWh}{m^2}\right)}{Yield\left(\frac{kg}{m^2}\right)} \quad (6)$$

Where:

$EUI\left(\frac{kWh}{m^2}\right)$ is the energy use intensity per floor area; and
$Yield\left(\frac{kg}{m^2}\right)$ is the average production of greenhouse fruits and vegetables.

To estimate the energy use intensity per floor area of a CEA facility in the Arctic, a building energy model of an indoor grow container and off-grid energy system was designed and modeled in TRNSYS18 (TESS, 2019), shown in Figure 4. The model is configured to run for one simulated year and operates under the following assumptions:

- The container and materials are located in the Arctic community of Cambridge Bay, Nunavut;

- Although lighting needs vary over a plant's growing cycle, a uniform light schedule is used throughout;
- Water pump electrical loads are neglected;
- Energy consumption and emissions involved with water delivery are ignored;
- Transportation emissions involved for replenishing grow media and nutrients are ignored;
- Crops are assumed to be perfectly irrigated and in ideal conditions for optimal yield; and
- Energy and emissions for equipment and supplies are neglected.

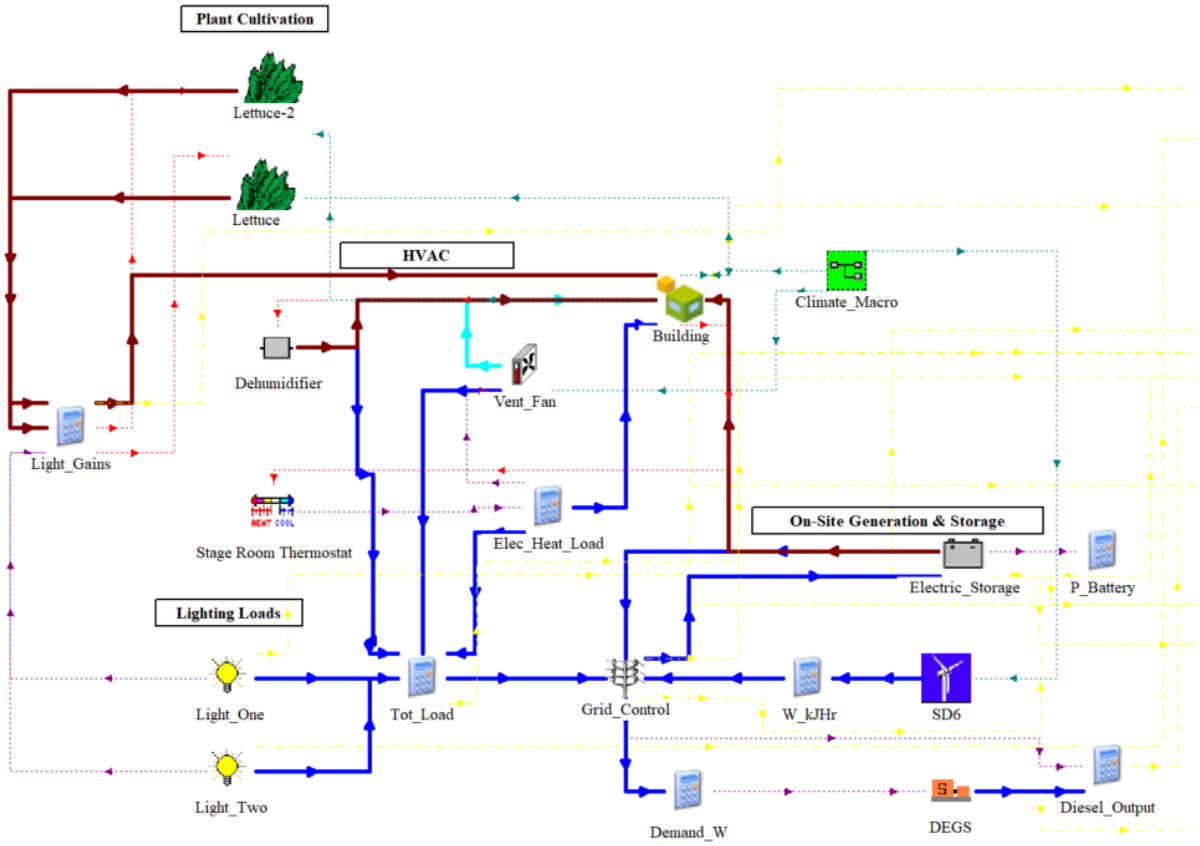

Figure 4. Overview of a Grow Container Model in TRNSYS18.

3.3.2.1 Configuration of the CEA facility

The configuration of the Arctic CEA facility that was modelled is shown in Figure 5. The indoor grow container is composed of two side-by-side 20 foot shipping containers with overall outside dimensions of 20' long x 16' wide x 8' 6" high. The left half of the layout contains equipment and supplies and the right half of the layout contains the grow area. The total cultivation area of the grow container is 216 ft^2 (20.1 m^2). The grow area is comprised of nine shelf racks, each with three levels of 8 ft^2.

The container has a south-facing 7’ 8” x 7’ 6” door and 2’ x 4’ triple-glazed window, as shown in Figure 6. The geometry was modeled using SketchUp (Trimble, 2022) and TRNSYS3D, a SketchUp plugin for TRNSYS to model multi-zone buildings. WINDOW 7.8 (Lawrence Berkeley National Lab, 2022) was used to determine the performance of the window, which was specified as having three layers of low emissivity 3 mm clear glass, with 12 mm gaps of 10% Air/90% Argon mix. A centre of glass U-value of 0.633 W/m^2·K and solar heat gain coefficient of 0.081 was determined and exported to the TRNSYS model along with a vinyl frame of U-Value of 1.7 W/m^2·K. The Sketchup geometry was imported into TRNBuild, a TRNSYS interface used to modify building model characteristics, to further develop the non-geometric properties of the building model. The components of the building were constructed by the layers detailed in Table 11 with the objective of maximizing insulation of the grow container, and finally, imported into TRNSYS as a Type 56 component.

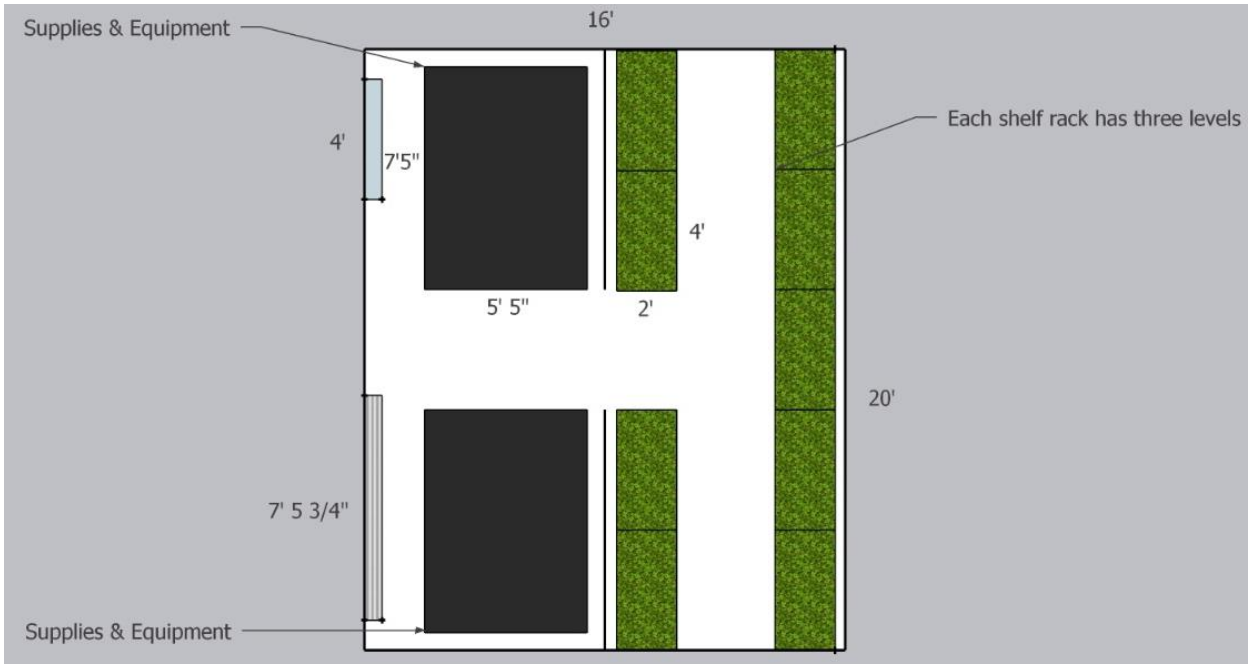

Figure 5. Proposed Configuration of Grow Container.

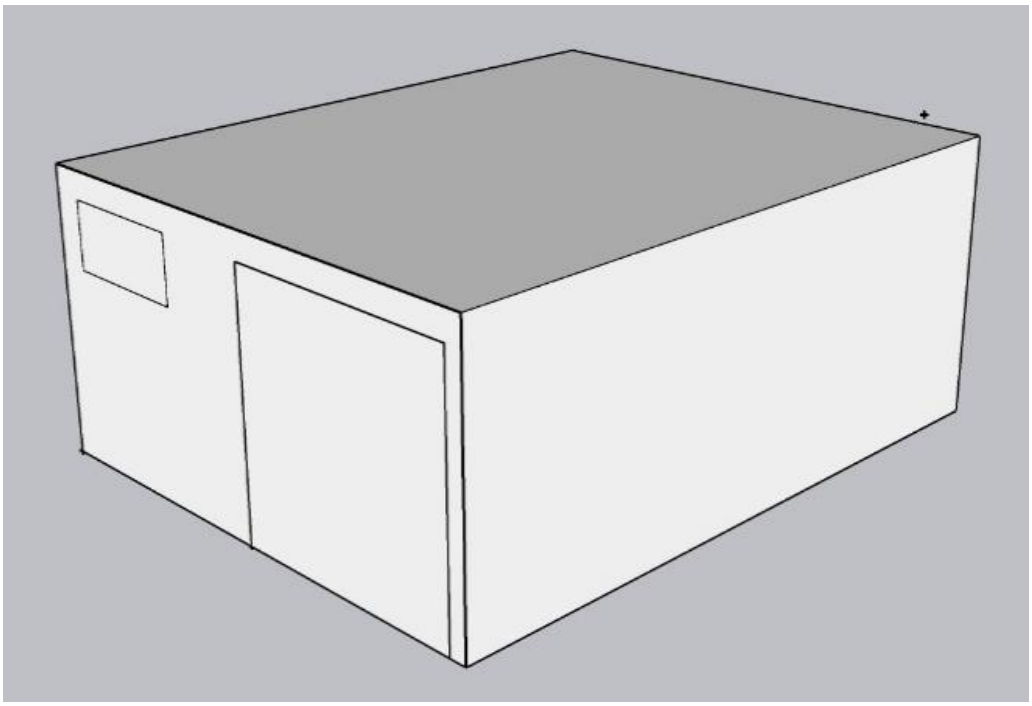

Figure 6. Isometric View of Grow Container Modeled in SketchUp.

Table 11. Construction materials of container.

Building Component	Layer (Exterior to Interior)	Material Property			Thickness [m]	Overall U-Value [W/m^2·K]	Convective Heat Transfer Coeffecient [kJ/h·m^2·K]	
		Conductivity [kJ/h-m-K]	Heat Capacity [kJ/kg-K]	Density [kg/m^3]			Inside	Outside
Wall	Steel	163	0.5	7824	0.002	0.227	22.5	120
	Polyisocyanurate	0.13	1.5	30	0.153			
Roof	Steel	163	0.5	7824	0.002	0.227	32.7	120
	Polyisocyanurate	0.13	1.5	30	0.153			
Floor	Terrazzo	6.48	0.79	2560	0.025	0.195	22.5	120
	Extruded Polystyrene	0.108	1.5	33	0.051			
	Plywood	0.432	1.21	544	0.019			
	Batt Insulation	0.18	0.96	19	0.147			
	Plywood	0.432	1.21	544	0.019			

3.3.2.2 HVAC system

The HVAC system includes a dual-stage electric resistance heater, a dehumidifier, and a 22.5 W variable-speed fan to control the ambient temperature, relative humidity, and ventilation of the container. The dehumidifier is modeled using a custom TRNSYS type and based on

empirical data for the ThermaStor Ultra-Aire XT150H Dehumidifier from Christen & Winkler (2009). The fan is modeled using Type 147 and varies from a minimum speed of 100 CFM, a first speed of 120 CFM, and a second speed of 140 CFM. The infiltration rate of outdoor air into the container is set to be a constant 0.21 ACH[1], aligning with the National Energy Code of Canada for Buildings regulation in NECB 2017: A-8.4.3.3.(3) (Codes Canada, 2017). The container's temperature is monitored and controlled by a stage room thermostat as detailed in Table 12. The controller is modeled using Type 108 and based on temperatures determined to be appropriate values for plant growth identified by literature of similar existing grow systems.

Table 12. Stage Room Thermostat Inputs and Values.

Thermostat Input	Temperature [ºC]
1st stage heating setpoint	18
2nd stage heating setpoint	15
1st stage cooling setpoint	23
2nd stage cooling setpoint	28

The container has seven electrical loads: the 22.5 W variable-speed fan, the electric space heater, the dehumidifier, LED grow lamps (48 fixtures at 70W each), a 27.7W circulation fan, a 240W load for data acquisition hardware and sensors, and 75W of standby power drawn from the inverter and rectifier. To minimize the lighting load, the lighting schedule follows a half on/half off cycle every twelve hours.

The heat gains of the container are contributed to by the container's electric space heating, the lighting loads, the plants' sensible and latent heat losses, and the battery, which is used for on-site energy storage and described further in Section **Error! Reference source not found.**. The sensible and latent heat gained from the plant is modeled using a custom TRNSYS type from Talbot & Monfet (2020).

3.3.2.3 Off-grid energy system

The CEA container's energy loads are met by the off-grid energy system shown in Figure 7. The base case for the analysis is all energy conversion being met by a small diesel generator. This case is very similar to community diesel generator systems meeting electricity demand in terms of emissions performance. A wind turbine and solar photovoltaic panels were also added to the system model to estimate the emissions reduction versus the base case. Battery energy storage is also considered in the system model. Each of these components are described in detail below.

[1] Assuming an air tightness of 1.0 ACH at ΔP = 50Pa and nominal ΔP = 5Pa.

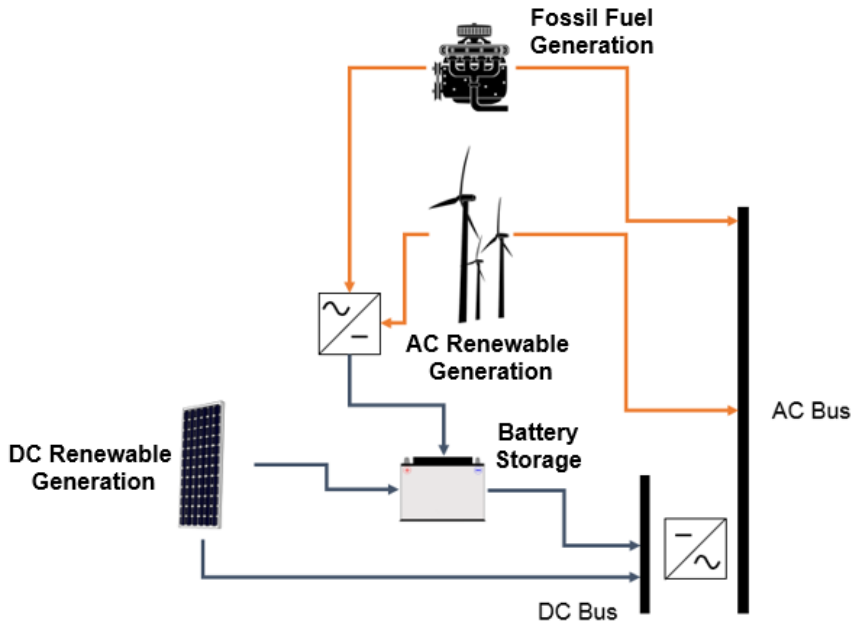

Figure 7. Off-grid energy system.

Diesel generator. The diesel generation system was modelled using TRNSYS standard library Type 120. This is a steady-state empirical performance map model. The model is constructed around a part-load ratio to fuel consumption rate curve. Based on input from project partners, a 7.6 kWe diesel generation system was to be installed at the site. Using manufacturer performance data (Hatz Diesel, 2020) the performance curve in Figure 8 was defined.

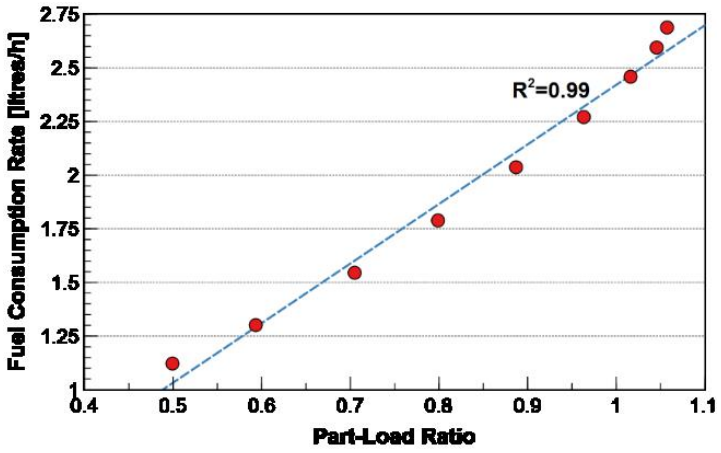

Figure 8. Diesel generator part-load versus fuel consumption, based on data from Hatz Diesel (2020).

The manufacturer reported fuel consumption in grams per kWh versus power output. To convert to the model required units of litres per hour shown in Figure 8, a diesel fuel density of 833

grams per litre was assumed (ISED, 2018). Figure 8 shows that the performance curve can be accurately approximated using a linear regression, with a coefficient of determination, R^2, of 0.99. While a second-order polynomial was found to more precisely capture the manufacturer reported data points in Figure 8, the model implementation is limited to linear expressions of performance curves. The salient model parameters are summarized in Table 13.

Table 13. Summary of diesel generator model parameters

Parameter	Value
Maximum electrical generation capacity [kW]	7.9
Minimum electrical generation capacity [kW]	3.9
Rated electrical generation [kW]	7.6
Performance curve slope [g/litre/PLR]	2.777
Performance curve intercept [g/litre]	-0.356

Operation of the diesel generator is governed by the grid controller, described below. For each time step, the controller passes a power demand to the diesel generator. If this demand is below the minimum operating threshold of the generator, the generator operates at its minimum output capacity and excess electrical generation is re-directed by the grid controller to either re-charge the battery system or an electrical load dump. Similarly, if demand exceeds maximum capacity, the generator operates at its maximum capacity point and additional energy is assumed to be drawn from an external electrical grid. The diesel generator is assumed to be housed in an enclosure which is separate from the agriculture container.

Wind Turbine. The wind turbine was modelled using TRNSYS standard library Type 90, which uses manufacturer reported test data to model turbine power output and performance under different environmental operating conditions. The power versus output curve under standard testing conditions forms the primary model for the turbine. The SD6 turbine is a three-blade horizontal axis turbine with a swept area of 23.7 m^2. Standard test data for the SD6 turbine was obtained from the Small Wind Certification Council (ICC-SWCC, 2019). Figure 9 plots the turbine power output versus wind speed at the hub height from ICC-SWCC (2019). The curve represents performance with a turbine inlet air density of 1.225 kg/m^3.

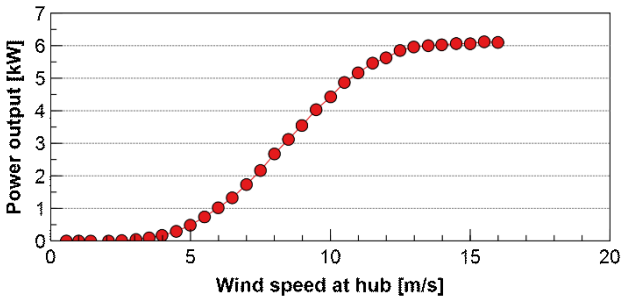

Figure 9. SD6 wind turbine power output versus wind speed at hub, data from ICC-SWCC (2019)

Climate inputs of wind speed, ambient dry-bulb temperature, and barometric pressure to the wind turbine model are obtained from the TRNSYS Type 15 “Weather” component. Table 14 provides a summary of the most pertinent wind turbine model parameters.

Table 14. Summary of wind turbine model parameters.

Parameter	Value
Rotor height [m]	9.0
Rotor diameter [m]	5.6
Rated power [kW]	5.2
Rated wind speed [m/s]	11.0

Solar Photovoltaic Panels. Solar photovoltaic (PV) panels were modelled using Type 190c, a validated empirical steady-state model of PV modules developed by Soto et al. (2006). This five-parameter model approximates system operating performance by representing PV modules as resistance-diode circuits. The panels modelled are based on 290 W modules from Canadian Solar (2018). The parameters used are listed below in Table 15.

Table 15. Summary of PV module model parameters.

Parameter	Value
Short-circuit current at STC, I_{SC} [A]	9.67
Open-circuit voltage at STC, V_{OC} [V]	39.3
Voltage at maximum power point and STC, V_{MPP} [V]	32.1
Current at maximum power point and STC, I_{MPP} [A]	9.05
Temperature coefficient of I_{SC} at STC [A/K]	0.004835
Temperature coefficient of V_{OC} at STC [V/K]	-0.11397
Number of cells wired in series	60
Extinction coefficient-thickness product of cover	0.013
Module area [m^2]	1.457
Five Parameters	
Ideality factor, a [-]	1.576
Light current, I_L [A]	9.682
Diode reverse saturation current, I_0 [A]	1.413E-10
Series resistance, R_s [Ω]	0.2735
Shunt resistance, R_{sh} [Ω]	219.2

Battery. The battery system was modelled using TRNSYS standard library Type 47, illustrated in Figure 4 as “Electric_Storage”. For the purposes of this study, the base transient energy balance algorithm is used. This approach uses a basic energy in, out, and stored balance as the simulation progresses. A constant charging efficiency is defined for the model to account for system energy transfer and storage inefficiencies. This parameter acts as a proxy for “round-trip” battery charge/discharge. It is realized as a loss in the model during charge of the battery

only; there is no constant standby loss during idle operation or losses during discharge. This is likely implemented in this way to simplify the simulation of transient operation and control of the battery.

Given the simplicity of the model, it may be considered agnostic to battery technology type. The charging efficiency was assumed to be 90% based on assumed round-trip efficiency of lithium-ion batteries reported by Brown (2018). The key battery model parameters are summarized in Table *16*.

Table 16. Summary of battery model parameters.

Parameter	Value
Cell energy capacity [Wh]	3000
Cells in parallel	1, 2, or 4
Cells in series	4
Charging efficiency [%]	90.0

Grid controller. A new grid controller model was developed for the micro-grid configuration shown in Figure 7. The grid control type acts as the central hub of the system energy model. At each simulation time step, AC and DC generation output, battery state-of-charge (SOC), and total site AC demand are taken as inputs to determine dispatch and control action. The grid controller algorithm also models the performance of the DC-to-AC inverter and AC-to-DC rectifier shown in Figure 7. Both devices are modelled assuming user-prescribed constant conversion efficiencies.

The first priority of the control algorithm was to supply all on-site renewable electricity generation to concurrent site demands. This choice was based on the philosophy that on-site generation is better utilized by directly supplying concurrent loads rather than being stored which incurs increased losses. If there is insufficient or no available renewable generation during a period of demand, the battery is discharged if there is sufficient capacity. Capacity is determined by the battery's SOC and also by a maximum power draw limit specified by the user. If there is no capacity in the battery to meet the load, or the demand is greater than the maximum the battery can provide, the battery is dispatched to provide the maximum power it is able to deliver and the remainder of the demand is requested from the diesel generator by the grid controller.

It was stated previously that the diesel generator can only be operated between minimum and maximum power outputs. The grid controller is aware of these limitations since these limits are passed to the controller as parameters. Therefore, if the request to the diesel generator is greater than the capacity of the generator, the controller accounts for this deficit by allocating that deficit to being supplied by an external source. If the demand is below the lower operating limit of the generator, the generator is set to run at its minimum operating point and the excess generation is used to charge the micro-grid battery system, illustrated as the connection between the fossil fuel generator and battery system via the rectifier in Figure 7. The controller parameters are summarized in Table 17.

Table 17. Summary of grid controller model parameters

Parameter	Value
High limit of battery SOC [%]	98
Low limit of battery SOC [%]	20
Battery output power capacity [kW]	10.8
Charge SOC threshold [%]	N/A
Inverter efficiency [%]	95
Rectifier efficiency [%]	95

The grid controller maintains a range of battery bank SOC based on the high and low limits described in Table 17. The high limit of 98% was implemented instead of 100% for numerical stability in the model. The low limit of 20% was selected to reflect a common 80% depth-of-discharge (DoD) used by manufacturers to rate the cycle life of the batteries. Battery output capacity was selected based on typical manufacturer-reported maximum continuous charge and discharge rates.

The charge SOC threshold was a parameter implemented in the control algorithm to include functionality present in the TRNSYS standard library grid controller Type 48. While not used in this simulation, this threshold can specify a limit where if the battery bank is below the SOC threshold and starts charging, then it must continue charging until the SOC of the battery meets the threshold. Otherwise, if the battery bank is discharging and passes below the threshold, it can keep discharging to its low limit of battery SOC. This enables an additional limit on deep discharge of the battery while still making capacity available during high periods of demand.

3.3.2.4 Plant Sensible and Latent Heat Balance Model

Stated previously in Section 3.3.2.2, the sensible and latent heat balance model from Talbot & Monfet (2020) was used simulate crops inside the CEA containter. Photosynthesis and respiration of crops introduces heat gains and losses within an enclosed space which impacts energy performance. Talbot & Monfet (2020) modelled lettuce growing in a building-integrated agricultural space and found that including or excluding the energy exchange from plants had a significant impact on results. Lavigueur (2022) developed a similar plant model also implemented in TRNSYS. They modelled tomatoes grown in a greenhouse, and compared modelled results to measured data from a greenhouse in Québec. They found that if they excluded the radiant and respiratory energy exchange from the plants the monthly heating loads were under-estimated.

For this study the model from Talbot & Monfet (2020) was used to simulate lettuce growing inside the CEA. The Leaf Area Index (LAI) was assumed to be 3.0 based on the recommendation for lettuce from Gramaans et al. (2017). LAI is a dimensionless parameter which represents the ratio of total one-sided leaf area per ground surface area. The Cultivation Area Cover (CAC) was assumed to be 90%, also per recommendations from Gramaans et al. (2017). CAC is a dimensionless parameter representing the ratio of total horizontal projection area of ground covered (shaded) by leaves to total cultivation area. The aerodynamic boundary

layer resistance of the lettuce was assumed to be 100 s/m per recommendations from Gramaans et al. (2017). Further details on the model parameters may be found in Monfet & Talbot (2020), Lavigueur (2022), or Gramaans et al. (2017).

As stated previously, the CEA was modelled as having a total cultivated area of 20.1 m^2 with the cultivated area split into two 10 m^2 zones. The LEDs for each zone operate with a 12 hour ON and 12 hour OFF cycle, with their cycles offset from each other by 12 hours. This control strategy mimics diurnal insolation and also reduces peak electrical demand. When the lights at ON they are assumed to emit a photosynthetically-active radiation (PAR) flux of 160 W/m^2. The corresponding Photosynthetic photon flux density (PPFD) of the LEDs is assumed to be 800 $\mu mol/s/m^2$, estimated from PPFD = 5 [$(\mu mol/s/m^2)/(W/m^2)$] * PAR as recommended by Gramaans et al. (2017).

3.3.3 Operational carbon emissions of CEA

In order to estimate the operational CO_2 emissions over a year of the container's operation, an emission factor, *EF* (kg CO_2e/kWh), is required, which varies according to the grid/fuel GHG intensity of the energy source. In this case, the liquid fuel consumption of the diesel generator was integrated to calculate the annual liquid fuel consumption intensity (L_{diesel}/kg of produce). This is then multiplied by the reported emission factor for diesel fuel (2.68 kg CO_2e/L_{diesel}) (Government of Canada, 2022) as shown in Equation (7).

$$Emission\ intensity\left(\frac{kg\ CO_2e}{kg\ Produce}\right) = EUI\left(\frac{L_{diesel}}{kg\ Produce}\right) \times EF\left(\frac{kg\ CO_2e}{L_{diesel}}\right) \quad (7)$$

4 Results and Discussion

This section presents the calculated carbon emissions from the two considered scenarios: delivering fresh produce from southern Canada via air transport and growing produce locally in a controlled environment. The total carbon emissions per kilogram of produce (kg CO_2e/kg of produce) was used as an indicator of the operational carbon emissions of the CEA facility. This indicator can be used to estimate the operational carbon emissions of such facilities, based on production data (kg or metric tons of fruits and vegetables). The emissions that were calculated for each scenario are presented below.

4.1 Air-Transported Produce Emissions

Since there are many different destination communities, two representative cases for importing produce to northern Canada were selected to form the basis of comparison based on consultation with flight personnel of the Aerospace Research Centre at NRC. The two representative northern communities selected are both in Nunavut: Iqaluit and Cambridge Bay.

4.1.1 Iqaluit, Nunavut

The first Arctic community selected for this emissions analysis is Iqaluit, Nunavut (YFB). The majority of produce transport for Iqaluit departs from the Hamilton, Ontario airport (YHM). The specific scenario analyzed was a round-trip flight from YHM to YFB by a Boeing 767-300 Freighter, a common cargo flight for transporting fresh produce to this location from southern Canada. Select technical characteristics of the 767-300 Freighter are reproduced in Table 18 (Boeing, 2014), while values for calculating the fuel burn for this trip are included in Table 19. Table 20 summarizes the fuel burn estimation calculations for a flight from YHM to YFB with a 767-300F. The landing and take-off values are taken from IPCC Guidelines on National Greenhouse Gas Inventories for a Boeing 767 (IPCC, n.d.).

Table 18. Technical characteristics of Boeing 767-300 Freighter aircraft.

Cargo Maximum Payload	52,700 kg
Cargo Total Volume	438 m^3
Maximum Fuel Capacity	90,770 L
Maximum Take Off Weight	185,060 kg
Maximum Range (max payload)	6,025 km
Typical Cruise Speed (at 35,000 feet)	850 km/h
Fuel burn rate (cruising)	4,940 kg/h

Table 19. Distance and time for calculating fuel burn for YHM to YFB

YHM to YFB great circle distance	2,404 km
Time duration of cruise and descent	2.83 h

Table 20. Fuel burned by flight component for YHM to YFB with Boeing 767-300F aircraft

Flight Component	Fuel burn rate	Amount	Fuel amount
Landing and take-off (IPCC, n.d.)	-	-	1,710 kg
Cruise	4,940 kg/h	2.83 h	13,980 kg
Total			15,690 kg

Given the maximum payload, cruising speed, and fuel burn amounts, the emissions intensity is approximately 21.0 kg CO_2e/km or 0.398 kg CO_2e/t·km or 0.956 kg CO_2e/kg produce. For the doubled distance of the YZF-YCB route, accounting for the return flight, this works out to

1.91 kg CO_2e/kg produce. Considering the assumptions listed, this emissions value serves as a lower bound of emissions for transporting produce to YFB.

4.1.2 Cambridge Bay, Nunavut

The second representative Arctic community selected for the analysis is Cambridge Bay, Nunavut. Cambridge Bay is located on Victoria Island, north of the Arctic coast of the Canadian mainland. Cambridge Bay lies about 2000 km due north of Regina, Saskatchewan and is serviced by Yellowknife, Northwest Territories, which is the closest major road-connected centre. Fresh food transport to Cambridge Bay is primarily by truck to Yellowknife from southern Canada and by air from Yellowknife (YZF) to Cambridge Bay (YCB). Since food originates from many different locations, both domestically and internationally, it is not possible to pick a single origin for food shipments. For the purposes of this analysis, Edmonton, Alberta will be used as the origin point, as it serves as an intermediate point for which shipments to Yellowknife by truck will pass through. The travelled road distance from Edmonton to Yellowknife is approximately 1,450 km. The great circle distance from YZF to YCB is 853 km.

For the doubled distance of the Edmonton-Yellowknife route, accounting for the return trip, the emissions for the surface transport works out to 165 kg/t or 0.165 kg CO_2/kg produce.

For many years, 737-200 jets served the route to the gravel runway of the Cambridge Bay Airport. This has recently changed due to the gravel-equipped 737-200 no longer being maintainable. ATR 42 aircraft now service the route as of 2023. The technical characteristics of the ATR 42-600 are listed in Table 21. As a significantly smaller aircraft than the 737-200 and 767-300, the ATR 42-600 serves as a valuable comparison of the food air transport emissions between larger and smaller aircraft.

Table 23 summarizes the fuel burn estimation calculations for a flight from YZF to YCB with an ATR 42-600. For the landing and take-off fuel burn listed in Table 23, a similar aircraft was used since the ATR 42 is not listed in the IPCC Guideline used for the Boeing 767 above. The SAAB 340 is also a twin-engine turboprop aircraft like the ATR 42, with weight and thrust values only slightly lower than the ATR 42. The LTO value for the SAAB 340 was scaled accordingly for the ATR 42-600 based on maximum take-off weights (MTOW).

Table 21. Technical characteristics of Boeing ATR 42-600 aircraft (ATR, 2023)

Maximum Payload	5,250 kg
Maximum Fuel Capacity	4,500 kg
Maximum Take Off Weight	18,600 kg
Maximum Range (max payload)	1,345 km
Typical Cruise Speed (at 19,685 feet)	535 km/h
Fuel burn rate (cruising)	620 kg/h

Table 22. Distance and time for calculating fuel burn for YZF to YCB

YZF to YCB great circle distance	853 km
Time duration of cruise and descent	1.59 h

Table 23. Fuel burned by flight component for YZF to YCB

Flight Component	Fuel burn rate	Amount	Fuel amount
Landing and take-off (IPCC, n.d.)	-	-	410 kg
Cruise and descent	620 kg/h	1.59 h	986 kg
Total			1,396 kg

Given the maximum payload, cruising speed, and fuel burn amounts, the emissions intensity is approximately 5.25 kg CO_2e/km or 1.00 kg CO_2e/t·km or 0.854 kg CO_2e/kg produce. For the doubled distance of the YZF-YCB route, accounting for the return flight, this works out to 1.71 kg CO_2e/kg produce.

Combined, the approximate transport emissions intensity for fresh food from Edmonton to Cambridge Bay is 1.88 kg CO_2e/kg produce, which is only slightly less than for Hamilton to Iqaluit at 1.91 kg CO_2e/kg produce due to the reduced air transport distance and increased ability to use surface transport, despite the less efficient aircraft. It is somewhat coincidental that these values are close, as the air transport emissions normalized by payload and distance for the Boeing 767-300F are about 40% that of the ATR 42-600.

4.1.3 Food Production Emissions in Southern Canada

The last step of the air transport emissions analysis is to include an emissions estimate for producing the food in a lower latitude location that would then be transported to the Arctic. A worst-case scenario was assumed in which the carbon emissions associated with field production of fruits and vegetables in the southern part of Canada is equal to the 2.1 kg CO_2e/kg produce. This corresponds specifically to the GHG emissions of tomatoes, which have the highest reported GHG emissions according to Poore and Nemecek (2018) (see Table 3). Thus, the total minimum estimated emissions from transporting fresh produce from southern Canada is around 4.01 kg CO_2e/kg produce for Iqaluit and 3.98 kg CO_2e/kg produce for Cambridge Bay. The actual emissions associated with this overall activity for each case will be greater due to the aspects that are neglected in this analysis.

4.2 Arctic Controlled Environment Agriculture Emissions

The energy model of the CEA facility was run for a total of 10 cases of wind, solar, and battery capacities, which are outlined in Table 24. The system is assumed to be off-grid due to current constraints with integrating renewable energy systems with local grids in small northern communities, but with advancing policies and infrastructure, it may be possible to deploy such a system to be grid-tied and export excess electricity to the local grid. Alternatively, as community-scale renewable energy nears more widespread deployment, there may be opportunities to make use of lower emissions electricity in the Canadian Arctic. However, at the same time, most remote communities are currently nearly 100% reliant on diesel fuel for electricity, so adding to the grid load even with renewable energy integrated could be seen as still causing additional diesel fuel to be combusted, particularly given the steady, constant load.

The base case (Case #1) for the analysis is all energy conversion being met by a small diesel generator. This case is very similar to community diesel generator systems meeting electricity demand in terms of emissions performance. The breakdown of annual demand by each load is shown in Figure 10, where it is clearly seen that the agriculture lighting is the majority of the demand at around 79%. As a result, the agriculture lighting offsets a major portion of what would be the heating demand and mitigating overheating with ventilation is necessary during the warmest months. The space heating system is the second highest demand at 13% and the data acquisition (DAQ) system is third at 5%.

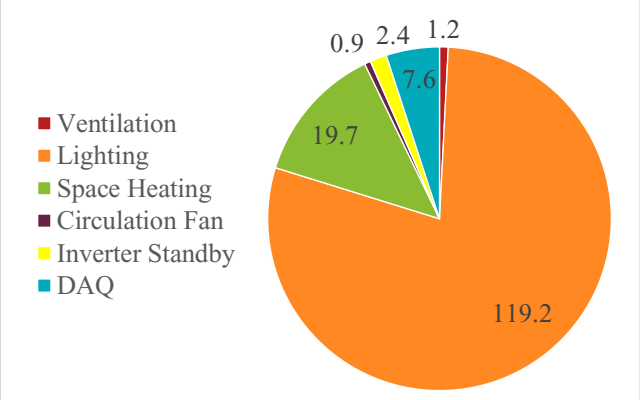

Figure 10. Annual load breakdown for the base case (Case #1) [GJ].

All 10 cases are arranged in Table 24 with increasing renewable energy capacity, and thus decreasing fuel use and emissions. As expected, the amount of renewable energy dumped begins to rise substantially as the combined wind turbine and solar PV capacity goes well above 10 kW. Due to the sustained load of the agriculture lights, the need for battery storage is relatively low unless the renewable energy system capacity is very large. This is illustrated by the minimal difference in performance between Cases #3, #4, and #5.

Table 24. Summary of GHG Emissions with Increasing Renewable Fraction

Case #	Wind Turbine [kW]	Solar PV [kW]	Battery [kWh]	Renewable Fraction	Wind Dumped	Solar Dumped	Annual Diesel Fuel [L]	Annual Emissions [kg CO_2e]
1	**-**	**-**	**24**	-	-	-	12,337	33,310
2	**5.2**	**-**	**24**	29%	2%	-	8,793	23,741
3	**5.2**	**5.8**	**12**	42%	5%	16%	7,118	19,219
4	**5.2**	**5.8**	**24**	43%	4%	10%	6,973	18,827
5	**5.2**	**5.8**	**48**	44%	2%	6%	6,851	18,498
6	**10.4**	**-**	**24**	46%	20%	-	6,670	18,009
7	**10.4**	**11.6**	**12**	60%	26%	53%	4,992	13,478
8	**10.4**	**11.6**	**24**	63%	24%	45%	4,575	12,353
9	**20.8**	**23.2**	**24**	73%	51%	78%	3,389	9,150
10	**20.8**	**23.2**	**48**	82%	48%	68%	2,187	5,881

Monthly electrical loads over the course of a year against a breakdown of the energy sources for the case of a single 5.2 kW wind turbine with 5.8 kW PV and 24 kWh of battery capacity (Case #4) are presented in Figure 11. This shows the minimal quantity of renewable energy dumped due to a sufficiently high stable load from the agriculture lighting relative to the capacities of the renewable energy system. The wind turbine meets 29% of the demand from the load, while only 4% is dumped. The solar PV meets 16% of the demand with only 10% dumped.

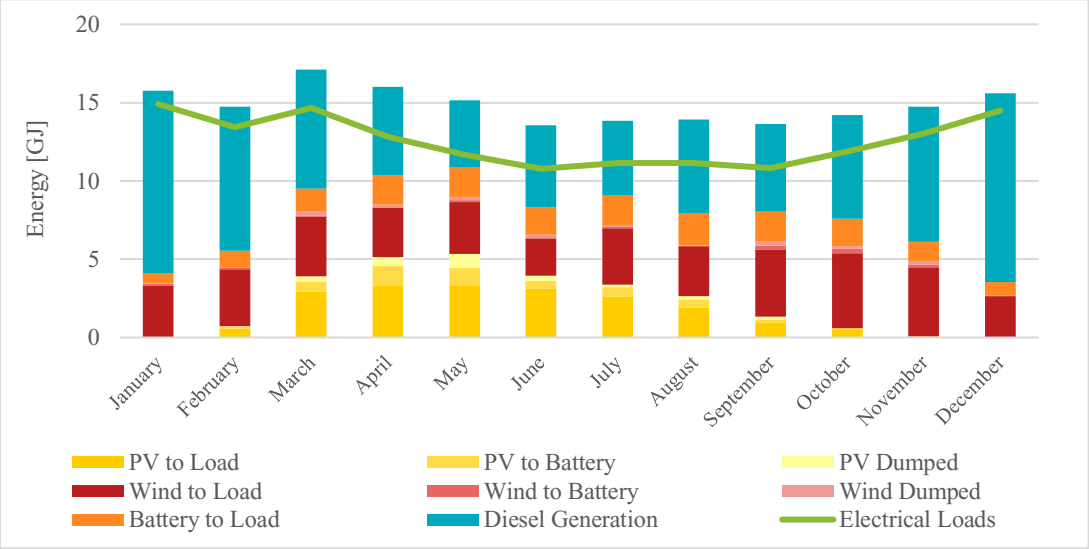

Figure 11. Monthly energy conversion and demand: 5.2 kW wind turbine, 5.8 kW solar PV, 24 kWh battery (Case #4).

Table 25 shows the CEA operational carbon emissions obtained for Case #4 and for the three different crop productivity estimates presented in the methodology. The range of emissions intensities is dramatic given that the productivities range by almost a full order of magnitude.

Table 25. CEA emissions sensitivity for different crop productivities for Case #4.

CEA emissions sensitivity			
Operational GHG emissions (kg CO_2e/year)	18,827		
Grow area (m^2)	20.1		
Crop type	Strawberries	Lettuce	Cucumber
Crop productivity (kg/m^2)	8	38	50
Emissions intensity (kg CO_2e/kg of produce)	117	25	19

The carbon emissions associated with the production of cucumbers in a CEA facility located in the Arctic are around nine times higher than those reported in the study by Stoessel et al. (2012), which is one of the few studies to report the carbon footprint of fruits and vegetables produced in fossil fuel heated greenhouses. This may be mainly due to the intensive use of fossil fuels in the Arctic for electricity generation, which highlights the importance of increasing the scale, efficiency and availability of clean energy for CEA facilities in the Arctic. As Dyer et al. (2011) suggested, research should aim at a higher ratio of yield to fossil fuel energy use, rather than simply trying to maximize greenhouse yields. This can be achieved through the use of renewable energy resources and more efficient production practices.

5 Summary and Conclusions

The total estimated emissions from transporting fresh produce by airplane from southern Canada is a minimum of 3.98 kg CO_2e/kg produce. In comparison, the CEA operational carbon emissions obtained for the base case of all energy conversion being met by a small diesel generator is around 33 kg CO_2e/kg for a crop productivity of 50 kg/m^2. This indicates that emissions from products produced locally in the Arctic in a CEA facility could be at least eight times the emissions compared to products shipped from southern Canada. This ratio becomes significantly greater for lower yielding crops. These results suggest that, at least from the perspective of mitigating greenhouse gas (GHG) emissions, CEA results in significantly greater emissions than flying in produce with the current level of dependence on fossil fuels for energy needs in Arctic Canada.

However, if renewable energy generation systems are used for CEA facilities, emissions can be reduced to a level similar to that of air-transported foods. This is evidenced in Case #10, which corresponds to the system with the largest installed capacity in terms of renewable energy systems (wind turbines and PV panels) and batteries. This case however, has a high fraction of electricity generated from renewable sources that is dumped if the system is not grid-tied. Interconnection to the local electricity distribution network would eliminate the dumping of renewable energy on this scale. This is of great importance as the installation and successful

operation of renewable energy systems in the Canadian Arctic can displace the electricity with the highest carbon emissions intensity in Canada, of around 800 g CO_2e/kWh for diesel generation (Environment and Climate Change Canada, 2022). This analysis has shown that without low carbon energy sources, the emissions from producing food in the Canadian Arctic with CEA are likely several times that of flying in food with air transport. It would take a very high fraction of clean energy supply to bring the emissions from CEA in the Canadian Arctic down to a level comparable with air transport of food from lower latitudes.

Acknowledgments

The authors acknowledge input from Anthony Brown from the NRC Aerospace Research Centre regarding flight calculations. The authors would also like to thank Marie-Hélène Talbot and Danielle Monfet from École de technologie supérieure for sharing their TRNSYS lettuce model for this study.

References

Air BP (2000). *Handbook of Products.* Accessed July 27, 2022 from https://web.archive.org/web/20110608075828/http://www.bp.com/liveassets/bp_internet/aviation/air_bp/STAGING/local_assets/downloads_pdfs/a/air_bp_products_handbook_04004_1.pdf

ATR (2023). *ATR 42-600.* Accessed April 20, 2023 from https://www.atr-aircraft.com/our-aircraft/atr-42-600/

Avard, E. (2015). *Northern greenhouses: An alternative local food provisioning strategy for Nunavik*. Doctoral dissertation, Université Laval.

Bamsey, M., Graham, T., Stasiak, M., Berinstain, A., Scott, A., Vuk, T. R., & Dixon, M. (2009). *Canadian advanced life support capacities and future directions*. Adv. Space Res., 44(2), 151-161.

Lages Barbosa, G., Almeida Gadelha, F. D., Kublik, N., Proctor, A., Reichelm, L., Weissinger, E., ... & Halden, R. U. (2015). *Comparison of land, water, and energy requirements of lettuce grown using hydroponic vs. conventional agricultural methods*. International journal of environmental research and public health, 12(6), 6879-6891.

Beshada, E., Zhang, Q., & Boris, R. (2006). *Winter performance of a solar energy greenhouse in southern Manitoba*. Canadian Biosystems Engineering, *48*(5), 1-8.

Boeing Company. (2008). *Fuel Conservation Strategies: Takeoff and Climb.* Accessed October 4, 2022 from https://www.boeing.com/commercial/aeromagazine/articles/qtr_4_08/article_05_3.html

Boeing Company. (2014). *Boeing 767-300F Backgrounder.* Accessed October 4, 2022 from https://www.boeing.com/farnborough2014/pdf/BCA/bck-767_5_13_2014.pdf

Bringer Air Cargo. (2021). *ATR-42.* Accessed April 20, 2023 from https://www.bringeraircargo.com/aircraft-types/atr-42/

Brown, M. D. (2018). *Simulation and Optimization of High-Penetration Wind and Solar Energy for the Canadian High Arctic Research Station*. Master's thesis, Carleton University.

Bucklin, R. A., Leary, J. D., Rygalov, V., Mu, Y., & Fowler, P. A. (2001). *Design parameters for Mars deployable greenhouses*. SAE Technical Paper Series 2001-01-2428.

Cairo Fruit. (2021). *Iceberg Lettuce.* Accessed April 20, 2023 from https://cairofruit.com/iceberg-lettuce/

Canadian Solar. (2018). *All-Black: CS6K-290|295|300MS*. Walnut Creek.

CBC News. (2022). *Inflation crisis: Soaring food prices in Canada's North prompting hunters to find new food sources*. Accessed April 17, 2023 from https://globalnews.ca/news/9035232/inflation-crisis-food-prices-northern-canada/

Chan, H. M., Fediuk, K., Hamilton, S., Rostas, L., Caughey, A., Kuhnlein, H., Loring, E. (2006). *Food security in Nunavut, Canada: Barriers and recommendations*. Int. J. Circumpolar Health, 65(5), 416-431.

Chau, J., Sowlati, T., Sokhansanj, S., Preto, F., Melin, S., & Bi, X. (2009). *Economic sensitivity of wood biomass utilization for greenhouse heating application*. Appl. Energy, 86(5), 616-621.

Chen, A., & Natcher, D. (2019). *Greening Canada's Arctic food system: Local food procurement strategies for combating food insecurity*. Canadian Food Studies, 6(1), 144–154.

Christensen, D., & Winkler, J. (2009). *Laboratory test report for ThermaStor Ultra-Aire XT150H dehumidifier (No. NREL/TP-550-47215)*. National Renewable Energy Lab.(NREL), Golden, CO (United States).

Clune, S., Crossin, E., & Verghese, K. (2017). *Systematic review of greenhouse gas emissions for different fresh food categories*. Journal of Cleaner Production, 140, 766-783.

Codes Canada. (2017). *National Energy Code of Canada for Buildings 2017*. Ottawa, ON, Canada: Codes Canada-NRC.

DSV. (n.d.). *Reefer container*. Accessed April 20, 2023 from https://www.dsv.com/en-ca/our-solutions/modes-of-transport/sea-freight/shipping-container-dimensions/reefer-container

Dyer, J. A., & Desjardins, R. L. (2018). *Energy use and fossil CO2 emissions for the Canadian fruit and vegetable industries*. Energy for Sustainable Development, 47, 23-33.

Dyer, J. A., Desjardins, R. L., Karimi-Zindashty, Y., & McConkey, B. G. (2011). *Comparing fossil CO2 emissions from vegetable greenhouses in Canada with CO2 emissions from importing vegetables from the southern USA*. Energy for Sustainable Development, 15(4), 451-459.

Dyer, J. A., & Desjardins, R. L. (2006). *An integrated index of electrical energy use in Canadian agriculture with implications for greenhouse gas emissions*. Biosystems Engineering, 95(3), 449-460.

Environment and Climate Change Canada (ECCC). (2022). *Emission Factors and Reference Values.* Retrieved July 15, 2022 from https://www.canada.ca/en/environment-climate-change/services/climate-change/pricing-pollution-how-it-will-work/output-based-pricing-system/federal-greenhouse-gas-offset-system/emission-factors-reference-values.html

Exner-Pirot, H., & Gulledge, J. (2012). *Climate change & international security: The Arctic as a bellwether. Center for Climate and energy solutions*. Centre for Climate and Energy Solutions.

Giroux, R., Berinstain, A., Braham, S., Graham, T., Bamsey, M., Boyd, K., Boucher, M. (2006). *Greenhouses in extreme environments: The Arthur Clarke Mars Greenhouse design and operation overview*. Adv. Space Res., 38(6), 1248-1259.

Great Circle Mapper (2023). http://www.gcmap.com/

Government of Canada. *Global warming potentials.* Retrieved July 27, 2022 from https://www.canada.ca/en/environment-climate-change/services/climate-change/greenhouse-gas-emissions/quantification-guidance/global-warming-potentials.html

Government of Canada. *Canada's Official Greenhouse Gas Inventory.* Retrieved July 15, 2022 from https://open.canada.ca/data/en/dataset/779c7bcf-4982-47eb-af1b-a33618a05e5b

Gramaans, L., van den Dobbelsteen, A., Meinen, E., Stanghellini, C. (2017). *Plant factories; crop transpiration and energy balance*. Agricultural Systems, 153, 138-147.

Guo, S., Tang, Y., Zhu, J., Wang, X., Yin, Y., Feng, H., Ai, W., Liu, X., Qin, L. (2008). *Development of a CELSS experimental facility*. Adv. Space Res., 41(5), 725-729.

Hatz Diesel. (2020). *Data sheet B-series*. Ruhstorf an der Rott.

ICC-SWCC. (2019). *Summary Report SWCC-11-04*. Retrieved from https://smallwindcertification.org/wp-content/uploads/2021/04/SWCC-11-04-Summary-Report-2020.pdf

Independent Electricity System Operator (2019). *Greenhouse Energy Profile Study.* Retrieved from https://www.ieso.ca/-/media/Files/IESO/Document-Library/research/Greenhouse-Energy-Profile-Study.ashx

International Air Transport Association (IATA). (n.d.). *Recommended practice 1678. CO_2 emissions measurement methodology.* Retrieved June 21, 2022 from https://www.iata.org/contentassets/34f5341668f14157ac55896f364e3451/rp-carbon-calculation.pdf

International Council on Clean Transportation. (2021). *CO_2 emissions from trucks in the EU: An analysis of the heavy-duty CO_2 standards baseline data.* Retrieved June 21, 2022 from https://theicct.org/publication/co2-emissions-from-trucks-in-the-eu-an-analysis-of-the-heavy-duty-co2-standards-baseline-data/

Intergovernmental Panel on Climate Change (IPCC). (n.d.). *Aircraft Emissions* in *Good Practice Guidance and Uncertainty Management in National Greenhouse Gas Inventories.* Retrieved April 25, 2023 from https://www.ipcc-nggip.iges.or.jp/public/gp/bgp/2_5_Aircraft.pdf

ISED. (2018). *Volume correction factors—diesel, bio-diesel and diesel blends*. Retrieved January 11, 2022, from https://www.ic.gc.ca/eic/site/mc-mc.nsf/eng/lm00127.html

Karenzi, J. (2020). *Development of Scalable Energy Distribution Models to Evaluate the Impacts of Renewable Energy on Food, Energy, and Water System Infrastructures in Remote Arctic Microgrids of Alaska*. Master's Thesis, University of Alaska Fairbanks.

Katzin, D., Marcelis, L. F., & van Mourik, S. (2021). *Energy savings in greenhouses by transition from high-pressure sodium to LED lighting*. Applied Energy, 281, 116019.

Kells, L., Kern, W.F., Bland, J.R. (1940). *Plane and Spherical Trigonometry*. McGraw Hill Book Company, Inc.

Lavigueur, C. (2022). *Improving greenhouse modelling in building performance simulation tools*. Master's Thesis, Polytechnique Montréal.

Lawrence Berkeley National Lab (2022). *WINDOW 7.8 and THERM 7.8*. https://windows.lbl.gov/therm-78-windows-78

Ljungqvist, H. M., Mattsson, L., Risberg, M., & Vesterlund, M. (2021). *Data center heated greenhouses, a matter for enhanced food self-sufficiency in sub-arctic regions*. Energy, 215, 119169.

McCartney, L., & Lefsrud, M. (2018). *Protected agriculture in extreme environments: a review of controlled environment agriculture in tropical, arid, polar, and urban locations*. Applied Engineering in Agriculture, 34(2), 455-473.

O'Flaherty, T., & Maher, M. J. (1987). *Evaluation of lining with PVC panels as a means of reducing heat loss from a glasshouse*. Irish Journal of Agricultural Research, 77-86.

Poore, J., & Nemecek, T. (2018). *Reducing food's environmental impacts through producers and consumers*. Science, 360(6392), 987-992.

Sambor, D. J., Wilber, M., Whitney, E., & Jacobson, M. Z. (2020). *Development of a tool for optimizing solar and battery storage for container farming in a remote Arctic microgrid*. Energies, 13(19), 5143.

Sipola, S. (2019). *From Community Gardens to Hybrid Hydroponics: The evolution of northern greenhouses and Arctic gardening*. Master's thesis, The Arctic University of Norway.

Soto, W. De, Klein, S. A., & Beckman, W. A. (2006). *Improvement and validation of a model for photovoltaic array performance*. Solar Energy, 80, 78–88.

Statistics Canada (2023). *Table 32-10-0025-01 Specialized greenhouse producers' operating expenses*. Accessed July 15, 2022 from https://www150.statcan.gc.ca/n1/en/catalogue/3210002501

Statistics Canada (2023). *Table 32-10-0456-01 Production and value of greenhouse fruits and vegetables*. Accessed July 15, 2022 from https://www150.statcan.gc.ca/t1/tbl1/en/tv.action?pid=3210045601

Stoessel, F., Juraske, R., Pfister, S., & Hellweg, S. (2012). *Life cycle inventory and carbon and water foodprint of fruits and vegetables: application to a Swiss retailer*. Environmental science & technology, 46(6), 3253-3262.

Talbot, M. H., & Monfet, D. (2020). *Estimating the impact of crops on peak loads of a Building-Integrated Agriculture space*. Science and Technology for the Built Environment, 26(10), 1448-1460.

Teitel, M., Shklyar, A., Segal, I., & Barak, M. (1996). *Effects of nonsteady hot-water greenhouse heating on heat transfer and microclimate*. J. Agric. Eng. Res., 65(4), 297-304.

TESS (2019). *TRNSYS: Transient System Simulation Tool.* https://www.trnsys.com

Trimble (2022). *SketchUp.* https://www.sketchup.com

WayBeyond and Agritecture Consulting (2021). *2021 Global CEA census report*. Accessed from https://engage.farmroad.io/hubfs/2021%20Global%20CEA%20Census%20Report.pdf

Zabel, P., Bamsey, M., Zeidler, C., Vrakking, V., Johannes, B.-W., Rettberg, P., Davenport, R. (2015). *Introducing EDEN ISS-A European project on advancing plant cultivation technologies and operations*. Proc. 45th Int. Conf. on Environmental Systems, 58, pp. 1-13. Bremen, Germany: The German Aerospace Center (DLR).

Zabel, P., Bamsey, M., Schubert, D., & Tajmar, M. (2016). *Review and analysis of over 40 years of space plant growth systems*. Life Sci. Space Res., 10, 1-16.

Zabel, P., Zeidler, C., Vrakking, V., Dorn, M., & Schubert, D. (2020). *Biomass production of the EDEN ISS space greenhouse in Antarctica during the 2018 experiment phase*. Frontiers in Plant Science, 11, 656.